Error Field Correction in Unstable Resistive Wall Mode (RWM) Regime

Y. In[1], G.L. Jackson[2], M. Okabayashi[3], M.S. Chu[2], J.M. Hanson[4], R.J. La Haye[2],
J.S. Kim[1], M.J. Lanctot[4], Y.Q. Liu[5], L. Marrelli[6], P. Martin[6], P. Piovesan[6], L. Piron[6],
H. Reimerdes[4], A. Soppelsa[6], E.J. Strait[2], and V. Svidzinski[1]

[1]FAR-TECH, Inc., San Diego, California 92121, USA
[2]General Atomics, San Diego, California 92186-5608, USA
[3]Princeton Plasma Physics Laboratory, Princeton, New Jersey 08543-0451, USA
[4]Columbia University, New York, New York, 10027-6902 USA
[5]Euratom/CCFE Fusion Association, Culham Science Centre, Abingdon, OX14 3DB, UK
[6]Consorzio RFX, Corso Stati Uniti 4, 35127, Padova, Italy

e-mail: yongkin@far-tech.com

Abstract. The simultaneous use of feedback control for error field correction (EFC) and stabilization of an unstable resistive wall mode (RWM) has been demonstrated in DIII-D. While the conventional EFC method addresses error fields in a pre-programmed manner, it is challenged when an unstable RWM becomes dominant, because a weakly stable or feedback-stabilized RWM becomes extremely sensitive to any small, uncorrected resonant error field. Since the DIII-D tokamak is uniquely equipped with internal coils for fast time response and external feedback coils for slower time response, independent magnetic feedback control in low and high frequency ranges allows us to explore the specific roles of EFC and direct feedback (DF) in active RWM control in *stable, marginal* and *unstable* RWM regimes. For an *unstable* RWM at the edge safety factor $q_{95}{\sim}3$, the simultaneous operation of DF with the internal coils and dynamic (feedback-controlled) EFC with the external coils enabled us not only to stabilize the unstable RWM but also to determine the necessary EFC in the presence of a feedback-stabilized RWM. The gain dependence of the feedback-stabilized RWM differs from those of stable and marginal RWMs. Recent experiments and modeling show that the gain increase at *stable* RWMs (at $q_{95}{\sim}5$ or 6) leads to the coil current increase, while a *marginal* RWM (at $q_{95}{\sim}4$) is insensitive to the feedback gains. In contrast, according to an analytic cylindrical model, the EFC in the unstable RWM regime is predicted to require high gain to approach the desired correction current. This is also consistent with numerical RWM feedback modeling using the MARS-F code. It has been shown that a choice of an "under-relaxation" factor with high feedback gain could achieve "fast-track" EFC, requiring far fewer iterations than the conventional EFC method. Broadband magnetic feedback beyond a wall characteristic frequency τ_w^{-1} enhanced the decay rates of resonant magnetic perturbations induced by various bursty MHD events, helping to create and sustain high-performance plasmas. The established methodology to determine the optimized EFC waveform with the simultaneous use of feedback control of EFC and DF is applicable for various operational scenarios with pressure beyond the no-wall ideal stability limit. In particular, it would be highly valuable when the onset of unstable MHD is sensitive to the quality of EFC.

1. Introduction

It is observed that a seemingly insignificant non-axisymmetric vacuum field (often called "error field") is not only amplified (proportional to β) in the presence of plasma, but also is closely tied with resistive wall mode (RWM)[1] stability [1]. (Here, β is defined as a ratio of plasma pressure to externally applied magnetic field pressure.) Although complete removal of such non-axisymmetric fields is impractical (if not impossible), the reduction of its adverse impact to the plasma is a prerequisite in order to achieve high-β plasmas in tokamaks.

Since the topology of the error field is overlapped with that of the RWM, the error field correction is usually provided by the same magnetic feedback control systems that have been developed for direct feedback stabilization on RWM in various toroidal devices (e.g. DIII-D, NSTX). Nonetheless, the roles of error field correction (EFC) and direct feedback (DF) stabilization on RWM in the magnetic feedback system are quite distinct; *the EFC is to minimize the lack of axisymmetry of external fields, while the DF stabilization on RWM is to*

---

[1]The RWM originates from an ideal external kink, whose growth is governed by the resistivity of the close-fitting wall [2]. Since the RWM often imposes the limit of the achievable maximum plasma pressure, RWM stabilization is essential for creating and sustaining high performance steady-state fusion plasmas.

nullify the magnetic perturbation originating from unstable RWM [3]. Thus, a clear distinction between EFC and DF can be made in terms of the bandwidth requirements, in that *the DF stabilization on RWM would require a broader bandwidth than the natural RWM growth rate γ_0 ($\sim \tau_w^{-1}$), while the EFC remains near-static in low frequency below τ_w^{-1}* [4]. Here τ_w is the characteristic time for magnetic perturbation to penetrate the resistive wall.

So far, the requirements for DF stabilization on RWM were clearly specified (for example in [4]), but the EFC strategy is not so straightforward, since it should be developed differently in consideration of various RWM regimes (*stable, marginal, and unstable*), as will be discussed here. For example, while the conventional EFC method (bandwidth < τ_w^{-1}) addresses error field in a pre-programmed manner, it is challenged when an unstable RWM becomes dominant, because a weakly stable or feedback-stabilized RWM becomes extremely sensitive to any small, but uncorrected resonant error field. Thus, in the unstable RWM regime, a pre-programmed EFC waveform that has been developed in stable RWM regime might not be valid, unless the additional subtleties necessary for RWM stabilization are taken into account. As a result, the only practical method in the unstable RWM regime is to use EFC and DF stabilization on RWM simultaneously, to make a feedback-stabilized RWM, and then to extract the optimized EFC waveform. The optimized EFC gains should be greater than twice the critical gain (G_{crit}) necessary for DF stabilization on RWM, as will be discussed later. The optimized EFC waveform is predicted to be achievable much faster, when we take advantage of an "under-relaxation" factor with high feedback gain. Although the feedback-controlled EFC would be mostly targeted for resonant magnetic perturbations in low frequency below τ_w^{-1}, broadband magnetic feedback covering a range of frequency beyond τ_w^{-1} enhances the decay rates of resonant magnetic perturbations often induced by various bursty MHD events, helping to create and sustain high-β plasmas. The details of each point will be addressed in the following sections.

In Sec. 2, the magnetic feedback control system in DIII-D is briefly described. In Sec. 3, the results of the simultaneous use of EFC and DF in unstable RWM regime [i.e. RWM at $q_{95}\sim3$, where q_{95} is the edge (95% normalized flux) safety factor] are presented. In Sec. 4, the subtleties of the EFC in *stable, marginal* and *unstable* RWM regimes are discussed based on both experimental data and theoretical models. In Sec. 5, a "fast-track" EFC strategy using 'relaxation factor' is discussed, based on an iterative EFC model. In Sec. 6, an advantage of broadband magnetic feedback application in high-β plasma is discussed.

2. Magnetic Feedback Control System in DIII-D

The DIII-D tokamak is uniquely equipped with internal coils ("I-coils") for fast time response and external feedback coils ("C-coils") for slower time response (limited by penetration through the vessel wall) [5], along with various poloidal and radial magnetic sensors, as schematically shown in Fig. 1. Thus, independent magnetic feedback control in low and high frequency ranges in DIII-D allowed us to explore the specific roles of EFC and DF in active RWM feedback control in various RWM regimes.
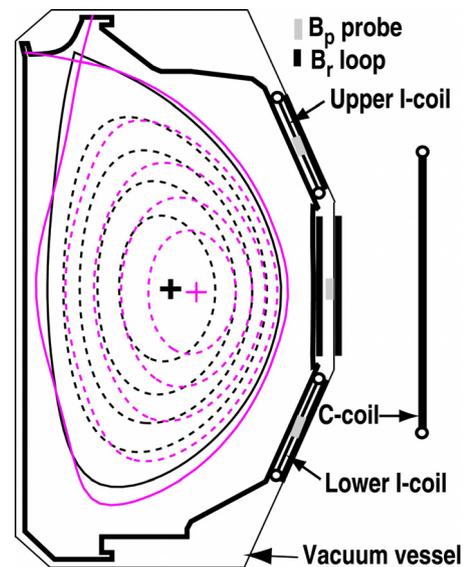

FIG. 1. Poloidal cross-section of low-β (in black) and high-β (in magenta) plasmas used for feedback-controlled EFC and RWM stabilization study in DIII-D. Shown are the upper single null (close to double-null) plasmas with magnetic sensors (poloidal field probes and radial field loops) and coils [internal (I-coils) and external (C-coils) to the vacuum vessel].

Typical plasma shapes of current-driven (in black) and pressure-driven (in magenta) RWM studies in this paper are overlaid in Fig. 1, where high-β plasma has a pronounced outward shift due to the Shafranov shift. Although the origin of the current-driven RWM in low-β plasma differs from that of the pressure-driven RWM in high-β plasma, there should be little or no difference in terms of the EFC strategy and DF stabilization on the RWM [4,6]. Unless otherwise specified in this paper, the magnetic sensors for feedback control are the outboard midplane poloidal sensors, while the I-coils are the primary feedback coils.

3. Simultaneous Use of EFC and DF Stabilization on Unstable RWM

Previously, the simultaneous feedback control for EFC and DF stabilization on RWM using both I-coils and C-coils was demonstrated in high-β plasmas in DIII-D [7,8]. However, since the stability boundary of the RWM in these high-β plasmas was greatly influenced by strong plasma rotation [9], as well as other kinetic effects (e.g. resonance with trapped fast ions moving in precession frequency or bounce frequency [10]), it remains unanswered whether active feedback control alone could have been sufficient in stabilizing the RWMs. In that regard, the application of active magnetic feedback control on current-driven RWMs convincingly demonstrated the effectiveness of the feedback algorithm, because neither rotation nor kinetic effects are influential on the current-driven RWMs in low-β ohmic plasmas [4].

Figure 2 shows the experimental results of the simultaneous operation of the EFC and DF using the internal and external coils. While the time evolution of the edge safety factor q_{95} remains similar [Fig. 2(a)], in one case an RWM at $q_{95} \sim 3$ occurs near $t = 590$ ms, terminating the discharge (black). In comparison, when the simultaneous operation of the dynamic EFC and DF is optimized (red), the RWM at $q_{95} \sim 3$ has been feedback-stabilized. As a result, the necessary EFC waveform in the unstable RWM regime, which cannot be found easily without feedback, can now be determined based on the low frequency EFC as shown in the red trace in Fig. 2(d). Hence, the simultaneous operation of DF with internal coils and dynamic (feedback-controlled) EFC with external coils enabled us not only to stabilize the unstable RWM but also to determine the necessary EFC in the presence of a feedback-stabilized RWM. Such simultaneous operation of dynamic EFC and DF could be the only practical method (if not the only way) to obtain the EFC waveform in the unstable RWM regime.
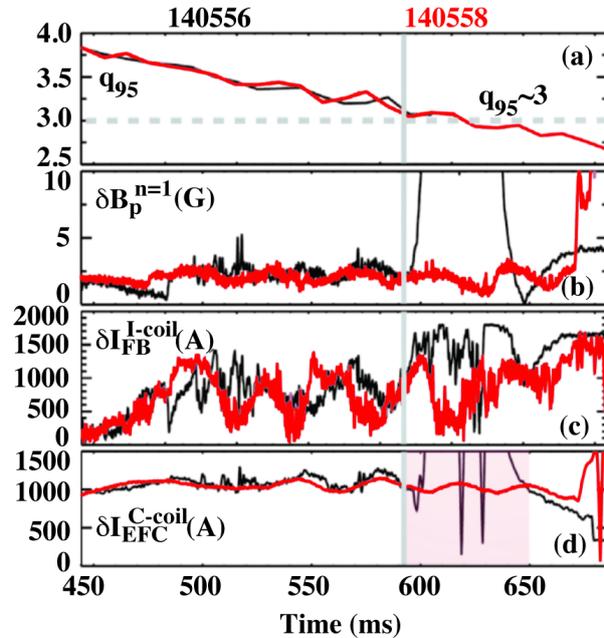

FIG. 2. Simultaneous operation of feedback-controlled EFC and DF on the unstable RWM at $q_{95} \sim 3$ with optimized gains (in red) and with lower gains (in black). Shown are the time traces of (a) edge safety factor q_{95}, (b) $n=1$ magnetic perturbations on poloidal field probes, (c) internal feedback coil currents, and (d) external EFC coil currents.

4. Subtlety of EFC in Stable, Marginal, and Unstable RWM Regimes

When the EFC is not sufficient, the DF, which originally aims at stabilizing an unstable RWM, is reacting to the need to correct the residual EF. However, depending on the RWM stability conditions (*stable, marginal and unstable*), the response of the magnetic feedback system to the need of additional EFC would be remarkably diverse.

Figure 3 shows the I-coil currents during a feedback gain scan with the pre-programmed (not feedback-controlled) C-coil EFC. Hence, the I-coil currents contribute to both DF and an additional EFC. It is clear from both experiment and modeling that the I-coil currents in the presence of stable RWMs (at q_{95}~5 or 6) increase with gain, while the I-coil currents with a marginal RWM (at q_{95}~4) are insensitive to the feedback gains [3]. But, according to a prediction of a cylindrical model developed by Okabayashi-Pomphrey-Hatcher (OPH model hereafter) [11], the EFC in unstable RWM regime requires high gain in order to approach the desired correction current [a normalized value of 1.0 in Fig. 3(c)]. Thus, the gain dependence of the feedback-stabilized RWM is predicted to be quite different from those of *stable* and *marginal* RWMs. The relationship between EFC and DF in various RWM regimes is consistent with a more rigorous RWM feedback modeling using the MARS-F code [6].

FIG. 3. *Stable, marginal and feedback-stabilized RWMs. Left: time traces of (a) edge safety factor q_{95}, and (b) internal feedback coil ("I-coil") currents at various gains (G_p=40, 80, 160 and 320 from the bottom respectively). In (c), the gain dependency of the I-coil currents varies subject to the RWM regimes, which is consistent with the predictions (dashed curves) of a cylindrical model [11].*

There are several important points regarding the EFC in various RWM regimes. First, the feedback-controlled EFC is always underestimating the required coil current in stable RWM regime, while overestimating it in unstable RWM regime. However, once the feedback gain is large enough, the EFC coil current in both stable and unstable RWM regimes converges to the desired coil current asymptotically. Second, the gain increase in the stable RWM regime leads to the feedback coil current increase. Since many of the tokamak operation scenarios belong to the stable RWM regime (unless unstable RWM regime is explored), the gain increase is often accompanied by coil current increase, leading to the saturation of the feedback-controlled coil currents. In a sense, a mere increase of gain without considering hardware limits may be more detrimental than a tolerable level of EFC in the operational point of view. Third, the gain increase in the unstable RWM regime is predicted to lead to the coil current decrease. So, unless the feedback gain is large enough, the overestimated EFC coil current is also likely to lead to the saturation of the coil current. Good examples of the gain dependent EFC iteration at low and high gains in DIII-D can be found in [12,13].

5.   "Fast-track" EFC Strategy

While it is clear that the feedback-controlled EFC would require high gain in either the stable or unstable RWM regime, a more practical question remains; *how quickly can an ideal pre-programmed EFC waveform be obtained?* Usually, many experimentalists prefer to use a pre-programmed EFC to exclude any possible influence of dynamic feedback action on their objectives in plasma experiments. However, since repeating the same plasma discharge only to find a proper EFC waveform is costly, it would be highly beneficial to minimize the number of iterations, if possible. In fact, there is such a "fast-track" EFC strategy that may allow us to reach the desired coil currents quickly, when an 'under-relaxation' factor is introduced [14].
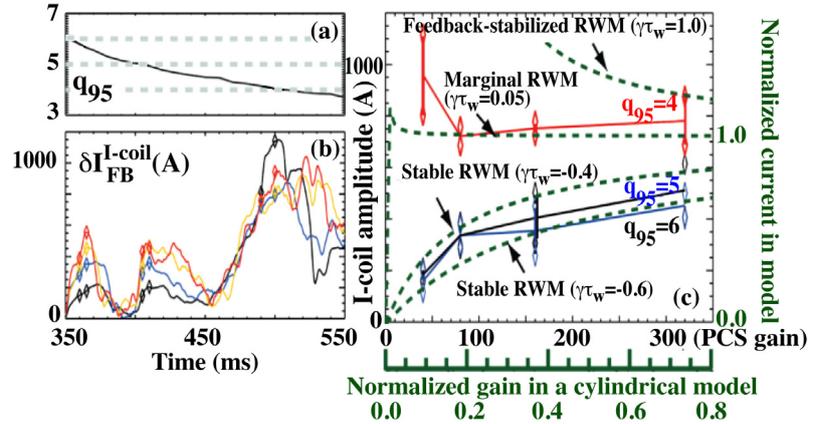
To understand the iterative EFC procedure, it helps to start with the OPH model [11]. The plasma (p), wall (w) and feedback coils (c) can be represented in lumped-circuit parameters as follows;

Plasma: $\quad L_{\text{eff}}\delta I_{\text{p}} + M_{\text{pw}}\delta I_{\text{w}} + M_{\text{pc}}(\delta I_{\text{c}} + \delta I_{\text{pre}} + I_{\text{err}}) = 0$ (1)

Wall: $\quad d[M_{\text{wp}}\delta I_{\text{p}} + L_{\text{w}}\delta I_{\text{w}} + M_{\text{wc}}(\delta I_{\text{c}} + \delta I_{\text{pre}} + I_{\text{err}})]/dt + R_{\text{w}}\delta I_{\text{w}} = 0$ (2)

Coil: $\quad \delta I_{\text{c}} = -G\delta\Psi$ (3)

with the plasma response defined as

$$\delta\Psi = A(I_{\text{err}} + \delta I_{\text{pre}} + \delta I_{\text{c}}) \quad , \tag{4}$$

where L and M are self- and mutual-inductances among plasma, wall and coil denoted by the subscripts of p, w, and c respectively, L_{eff} characterizes the plasma with the RWM stability condition as discussed in [11], A is the plasma amplification, I_{err} is the current equivalent to unknown error field, δI_{pre} is the pre−programmed coil current, δI_{c} is the feedback coil current, and R_{w} is the resistance of the wall [12]. Here the mutual inductances associated with I_{err} and δI_{pre} with plasma and wall are assumed to be the same as those associated with δI_{c}. Thus, the feedback-controlled coil current in a closed-loop leads to

$$\delta I_{\text{c}} = c\,(I_{\text{err}} + \delta I_{\text{pre}}) \quad , \tag{5}$$

where $c = -1/(1/GA + 1)$. As G_{crit} is the gain necessary to stabilize the unstable RWM, no more eddy current ($\delta I_{\text{w}}=0$) associated with the unstable RWM would flow on the resistive wall at $G=G_{\text{crit}}$. Thus, removing the term δI_{w} in Eq. (1) gives a relationship between δI_{p} and δI_{c}, so that

$$\delta I_{\text{p}} = -(M_{\text{pc}}/L_{\text{eff}})(\delta I_{\text{c}} + \delta I_{\text{pre}} + I_{\text{err}}) \quad . \tag{6}$$

Assuming that the error field (I_{err}) has been fully corrected by the pre-programmed current (δI_{pre}), the pure plasma response ($\delta\Psi = \delta I_{\text{p}}$) to δI_{c} at $G=G_{\text{crit}}$ can be found in combination of Eqns (3) and (4). Thus, the critical gain G_{crit} is ($L_{\text{eff}}/M_{\text{pc}}$), which is the inverse of the plasma amplification $-1/A$. Now, the parameter c in Eq. (5) can be rewritten as $c = 1/(G_{\text{crit}}/G-1)$, while the unstable RWM is characterized by $L_{\text{eff}} > 0$ (i.e. $G_{\text{crit}} > 0$).

Suppose that a choice of gain is fixed and that the superscript for each quantity based on Eq. (5) denotes the number of iteration, no iteration leads to $\delta I_{\text{pre}}^{(0)} = 0$, $\delta I_{\text{c}}^{(0)} = cI_{\text{err}}$. Then, the pre-programmed current at the 1st iteration $\delta I_{\text{pre}}^{(1)}$ is determined by $\delta I_{\text{c}}^{(0)}$, so that $\delta I_{\text{pre}}^{(1)} = \delta I_{\text{c}}^{(0)} = cI_{\text{err}}$, while the feedback coil current at the 1st iteration leads to $\delta I_{\text{c}}^{(1)} = c(I_{\text{err}} + cI_{\text{err}}) = cI_{\text{err}}(1+c)$. At the 2nd iteration, the $\delta I_{\text{pre}}^{(2)}$ will be the sum of $\delta I_{\text{pre}}^{(1)}$ and $\delta I_{\text{c}}^{(1)}$, so that $\delta I_{\text{pre}}^{(2)} = \delta I_{\text{pre}}^{(1)} + \delta I_{\text{c}}^{(1)} = c\,I_{\text{err}} + c\,I_{\text{err}}(1+c) = c\,I_{\text{err}}\,\{1+(1+c)\}$, while $\delta I_{\text{c}}^{(2)} = c\,[I_{\text{err}} + cI_{\text{err}}\{1+(1+c)\}] = c\,I_{\text{err}}\,(1+c)^2$. Similarly, at the n-th iteration, as long as $|1+c| < 1$ is satisfied, the pre-programmed coil current $\delta I_{\text{pre}}^{(n)}$ converges to

$$\delta I_{\text{pre}}^{(n)} = \sum_{i=0}^{n-1} \delta I_{\text{c}}^{(i)} = cI_{\text{err}}\left[\sum_{i=0}^{n-1}(1+c)^i\right] = cI_{\text{err}}\frac{1-(1+c)^n}{1-(1+c)} = -I_{\text{err}}\left[1-(1+c)^n\right] \quad . \tag{7}$$

and $\delta I_c^{(n)}$ leads to

$$\delta I_{\text{c}}^{(n)} = c\,I_{\text{err}}(1+c)^{\text{n}} \quad . \tag{8}$$

It is important to notice that the convergence criterion for pre-programmed coil current requires
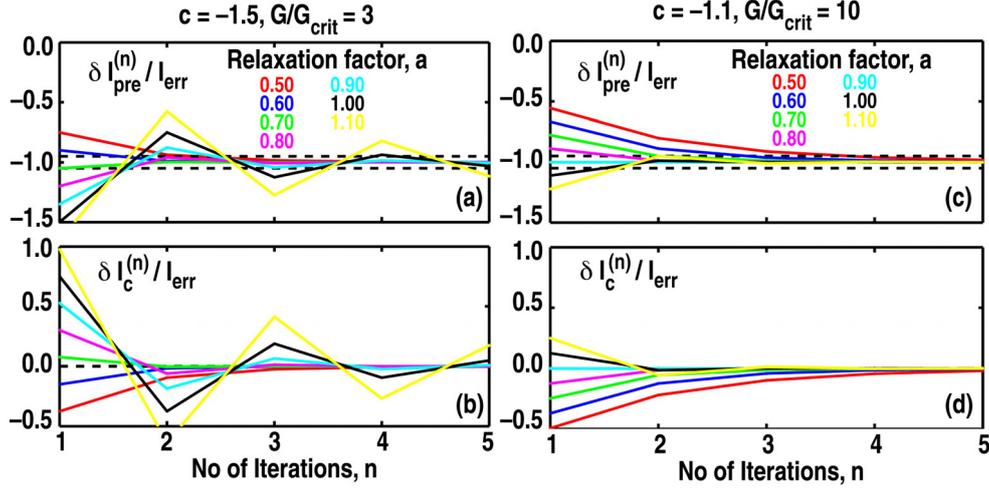
$$\left|1+c\right| < 1 \quad . \tag{9}$$

FIG. 4. *Pre-programmed EFC coil currents δI_{pre} and feedback coil currents δI_c normalized to error field I_{err} vs no. of iterations at various relaxation factors in model. In (a) and (b), a low gain ($G/G_{crit}=3$) is considered, while in (c) and (d), a high gain ($G/G_{crit}=10$) is under consideration. The dashed lines in (a) and (c) are the target area within ±5% uncertainty, while those with $\delta I_c = 0$ in (b) and (d) are the ideal targets.*

This leads to $-2 < c < 0$. So, $G/G_{crit} > 2$, since $c = 1/(G_{crit}/G-1)$. In the unstable regime ($L_{eff}>0$), since $G_{crit} > 0$, G is required to satisfy

$$G > 2G_{crit} \quad . \tag{10}$$

As the EFC logic is always set to be in negative feedback as defined in Eq. (3), this suggests the feedback-controlled EFC gain should be larger than $2G_{crit}$.

To improve the convergence of the solution further, a relaxation factor a can be introduced (See e.g. Ref. [14]). Specifically, the pre-programmed current $\delta I_{pre}^{(i+1)}$ at *(i+1)*-th iteration can be adjusted with a relaxation factor a, $(0<a<2)$ as follows;

$$\delta I_{pre}^{(i+1)} = \delta I_{pre}^{(i)} + a\left[\delta I_{TARGET}^{(i)} - \delta I_{pre}^{(i)}\right] = \delta I_{pre}^{(i)} + a\delta I_c^{(i)} \tag{11}$$

where $\delta I_{TARGET}^{(i)}$ is the total current found at *i*-th iteration ($=\delta I_{pre}^{(i)} + \delta I_c^{(i)}$). Similarly to the steps shown above, at the *n*-th iteration, as long as $|1+ ac| < 1$ is satisfied, the pre-programmed coil current $\delta I_{pre}^{(n)}$ converges to

$$\delta I_{pre}^{(n)} = acI_{err}\left[\sum_{i=0}^{n-1}(1+ac)^i\right] = acI_{err}\frac{1-(1+ac)^n}{1-(1+ac)} = -I_{err}\left[1-(1+ac)^n\right] \tag{12}$$

and $\delta I_c^{(n)}$ leads to

$$\delta I_c^{(n)} = cI_{err}(1+ac)^n \quad . \tag{13}$$

Now, the convergence condition becomes $|1+ac| < 1$, instead of $|1+ c| < 1$. The convergence condition can be simplified to

$$G > G_{crit}\left[2/(2-a)\right] \quad . \tag{14}$$

Thus, when $a=1$, the convergence condition in Eq. (10) is recovered. The use of under-relaxation ($0 < a < 1$) leads to convergence improvement, while that of over-relaxation ($1 < a < 2$) can result in speedy convergence [14]. Thus, depending on the choice of relaxation factor, the convergence criterion of Eq. (10) can be also relaxed in the neighborhood of $2G_{crit}$, resulting in different EFC gain constraints.

Figure 4 shows the pre-programmed EFC coil current $\delta I_{pre}^{(n)}$ and feedback coil current $\delta I_c^{(n)}$ normalized with the desired EF I_{err} with various relaxation factors at low (G/G_{crit}=3) and high (G/G_{crit}=10) gain cases, based on Eqns (12) and (13). Assuming that the EFC within $\pm5\%$ uncertainty is satisfactory [as dashed lines in Fig. 4(a,c)], the number of iterations at high gain [Fig. 4(c)] is substantially reduced in comparison with that at low gain [shown in Fig. 4(a)]. For example, based on the conventional EFC (a=1), at least 5 iterations are required at the low gain (G/G_{crit}=3), while 2 iterations are sufficient at the high gain (G/G_{crit}=10). However, if a decent range of "under-relaxation" factors [e.g. 0.6–0.8] are used at the low gain (G/G_{crit}=3), the required number of iterations is no more than 2 iterations. Moreover, at the high gain (G/G_{crit}=10), a good choice of "under-relaxation" factor [e.g. a=0.9 in Fig. 4(c,d)] is selected, only one iteration would be sufficient. Although an 'over-relaxation' factor can also reduce the number of iterations at high gain [e.g. a=1.1 in Fig. 4(c,d)], there could be a convergence issue in particular at low gain [e.g. a=1.1 in Fig. 4(a,b)]. Therefore, a prudent choice of "under-relaxation" factor with high feedback gain would help us reach "fast-track" EFC, which requires far fewer iterations than the conventional (a=1) iteration scheme.

6. Broadband Magnetic Feedback in High-β Plasmas

In DIII-D, it is routine to provide high-quality EFC to minimize the resonant n=1 components. While the understanding of the EFC and DF in various RWM regimes is being enhanced using low-β plasmas, the ultimate application of this study lies in the support of high-β plasmas that could exceed the no-wall stability limit, while robustly suppressing pressure-driven RWMs. Figure 5 shows a comparison of such high-β ($\beta_N > 3$) plasmas with: i) loss of EFC (black, 142346 from t ~ 3500 ms), ii) conventional EFC with low frequency feedback (bandwidth $< \tau_w^{-1}$) (red, 141583), and iii) broadband (bandwidth $\gg \tau_w^{-1}$) magnetic feedback (magenta, 142347), whose typical plasma shape was already compared with that of low-β plasma in Fig. 1. When no feedback (in black) was provided (because of the power supply trip near t ~ 3500 ms), the baseline of the resonant n=1 components $\delta B_p^{n=1}$ was elevated to ~10 G as shown in Fig. 5(c). [Despite the loss of EFC (in black, Fig. 5), the high-β discharge survived likely due to strong plasma rotation, which was reduced somewhat but might have been high enough to prevent the resonant fields from seeding magnetic islands inside the
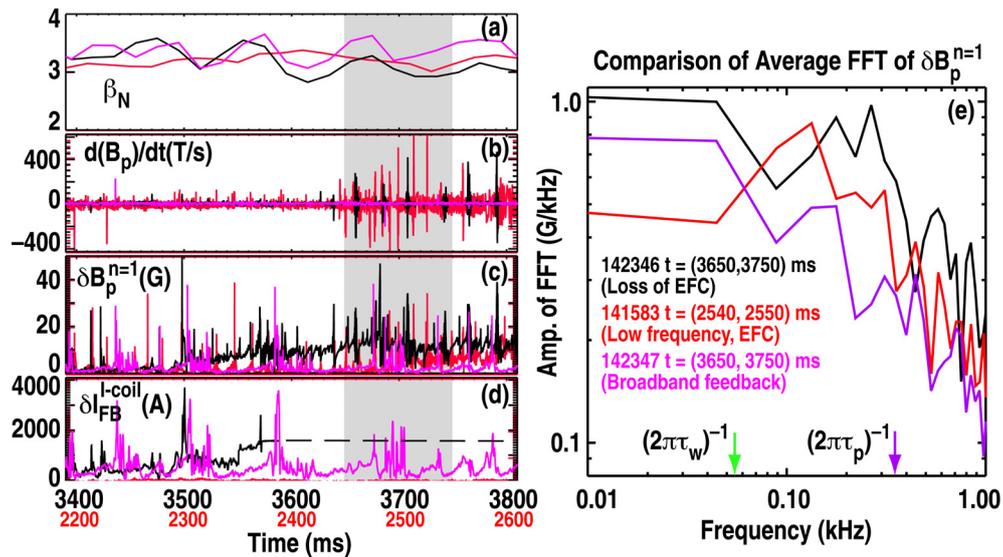

FIG. 5. Bandwidth-dependent magnetic feedback in high-β plasmas. Shown on the left are the time traces of (a) normalized–β, β_N, (b) poloidal Mirnov, (c) n=1 magnetic perturbation, and (d) I-coil feedback coil currents, while shown on the right is (e) the comparison of averaged FFT of $\delta B_p^{n=1}$ marked in the shaded time period of (c) with fishbones. It is to be noted that the discharge 141583 (in red) is in different time base, while the other discharges, 142346 (in black) and 142347 (in magenta), are synchronized with the same time bases.

plasma.] Had there been a feedback-controlled EFC current of ~1.5 kA as drawn in the dashed line in Fig. 5(d), the elevated baseline of the resonant components could have vanished. In fact, the δI_{FB}^{I-coil} for the other two discharges (with low-frequency EFC and broadband magnetic feedback) in Fig. 5(d) show the additional EFC only, where the pre-programmed current of ~1.5 kA was being delivered to remove the "near-static" error field that might have been the same level as shown in the case of the loss of EFC.

Since the primary purpose of EFC is to minimize any non-axisymmetric EF, the EFC-quality can be evaluated based on the performance of how effectively the $n=1$ resonant components, including uncorrected resonant EF, are eliminated or mitigated. For example, the fishbone-instabilities [as distinctively characterized in the shaded region of Fig. 5(b)] comprise $n=1$ resonant components in a wide range of frequency, which is much higher than τ_w^{-1}. A comparison of the fast-Fourier-transformation (fft)-based mode spectra of $\delta B_p^{n=1}$ shows the performance of the bandwidth-dependent magnetic feedback at least qualitatively, though a rigorous quantitative comparison in terms of bandwidth should be made with the growth and decay rates of each burst. While the low frequency EFC (red) substantially reduces the level of $\delta B_p^{n=1}$, broadband magnetic feedback (magenta) shows much lower level of $\delta B_p^{n=1}$ within the bandwidth [marked with an arrow at $(2\pi\tau_p)^{-1}$, where τ_p is the feedback time constant which imposes the bandwidth of feedback system], suggesting that the duration of the $n=1$ resonant components (e.g. driven by fishbones) would be reduced significantly due to broadband magnetic feedback. [As a note, the time constant τ_p of low frequency EFC (not broadband magnetic feedback) is much longer than τ_w, so that $(2\pi\tau_p)^{-1}$, which resides out of the range of the horizontal axis of Fig. 5 (e), is not shown. Also, the onsets of the fishbones were not affected by the broadband magnetic feedback.] Overall, when EFC quality is critical at high-β plasma due to a threat of neoclassical tearing modes and RWMs, broadband magnetic feedback would be an effective tool in enhancing the decay rates of the resonant components driven by various bursty MHD events, as well as in providing the necessary EFC and DF on RWM.

References

[1]   BOOZER, A.H., Phys. Rev. Lett. **86** (2001) 5059
[2]   FREIDBERG, J.P., *Ideal Magnetohydrodynamics*, Plenum Pres, New York (1987)
[3]   IN, Y., *et al.*, Nucl. Fusion **50** (2010) 042001
[4]   IN, Y., *et al.*, Plasma Phys. Control. Fusion **52** (2010) 104004
[5]   STRAIT, E.J., *et al.*, Phys. Plasmas **11** (2004) 2505
[6]   LIU, Y., *et al.,* Phys. Plasmas **17** (2010) 072510
[7]   GAROFALO, A.M., *et al.*, Phys. Plasmas **13** (2006) 056110
[8]   OKABAYASHI, M., *et al.*, Nucl. Fusion **45** (2005) 1715
[9]   BONDESON, A. and WARD, D.J., Phys. Rev. Lett. **72** (1994) 2709
[10] HU, B. and BETTI, R., Phys. Rev. Lett. **93** (2004) 105002
[11] OKABAYASHI, M., *et al.*, Nucl. Fusion **38** (1998) 1607
[12] OKABAYASHI, M., *et al.*, "Error field correction in stable/unstable RWM regime—a view of dynamic error field correction," Proc. of 15th Meeting of the ITPA MHD Stability Topical Group, 2010, National Institute for Fusion Science, Toki, Japan.
[13] REIMERDES, H., *et al.,* "Error Field Tolerance and Error Field Correction Strategies for ITER," submitted to Fusion Science and Technology (2010)
[14] PRESS, W.H., *et al.*, *Numerical Recipes*, 2nd Ed., Cambridge University Press, Cambridge (1992)